

Short Communication

Study on Corrosion Protection of Q235 Steel in Simulated Soil Pore Solution by Different Electrodeposited Coatings

Junwen Zou¹, Zhoufeng Zhao^{2,*}, Jie Zhang², Zhen Zhou¹, Sheng Xu¹, Bo Ye¹, Jun Zhang³

¹ Zhejiang Electric Power Boiler Pressure Vessel Inspection Institute Corporation Limited, Hangzhou 310014, China;

² Electric Power Research Institute of State Grid Zhejiang Electric Power Corporation Limited, Hangzhou 310014, China;

³ School of Power & Mechanical Engineering, Wuhan University, Wuhan 430072, China;

*E-mail: tdecastro@126.com

Received: 8 November 2022 / Accepted: 12 December 2022 / Published: 27 December 2022

Q235 steel as power grounding material was selected as the substrate, and different coatings (Zn-Ni alloy coating, Zn-Ni-W alloy coating and Zn-Ni-W/ZrO₂ composite coating) were electrodeposited on its surface. The corrosion behavior of Q235 steel and different electrodeposited coatings in simulated soil pore solution was investigated through electrochemical testing. The results show that Zn-Ni alloy coating, Zn-Ni-W alloy coating and Zn-Ni-W/ZrO₂ composite coating can inhibit the corrosion process of Q235 steel in simulated soil pore solution to improve its corrosion resistance. The phase composition of Zn-Ni-W alloy coating is the same as that of Zn-Ni alloy coating, while Zn-Ni-W/ZrO₂ composite coating contains Zn phase, Ni₅Zn₂₁ phase and ZrO₂ phase. ZrO₂ particles are uniformly doped in the composite coating. Compared with Zn-Ni alloy coating and Zn-Ni-W alloy coating, Zn-Ni-W/ZrO₂ composite coating has the lowest corrosion current density (9.87×10^{-7} A/cm²) and the highest charge-transfer resistance (7.34×10^3 Ω·cm²). After being corroded by 15 mA DC stray current for 14 days, it still maintains integrity and high compactness with lightest corrosion degree. Electrodeposition of Zn-Ni-W/ZrO₂ composite coating can not only meet the electrical conductivity requirements of power grounding electrode, but also significantly improve the corrosion resistance of carbon steel grounding electrode under the combined action of electrochemical corrosion and stray current corrosion in soil.

Keywords: Power grounding material; Corrosion protection; Electrodeposition; Zn-Ni alloy coating; Zn-Ni-W alloy coating; Zn-Ni-W/ZrO₂ composite coating

1. INTRODUCTION

Grounding plays an important role in ensuring the safe operation of power transmission and distribution system. The common grounding materials are carbon steel, copper, stainless steel,

aluminum alloy, and so on [1-3]. Carbon steel is widely used as grounding material because of its obvious advantages, such as low price, good mechanical performance, excellent ductility, and so on. However, the carbon steel buried in soil for a long time, is subjected to electrochemical corrosion of soil pore solution and stray current corrosion caused by discharge from power grid operation, which usually shows loose and porous surface with severe local damages. It can be said that corrosion of grounding material has become one of the most prominent problems in power transmission system [4-6]. Therefore, it is necessary to take measures to improve the corrosion resistance of carbon steel as power grounding material, so as to reduce the influence of electrochemical corrosion and stray current corrosion of soil pore solution on its service life.

In view of the requirement of stable conducting electricity for grounding material, the surface treatment can not only meet the requirements of stable conducting electricity of carbon steel as power grounding material, but also achieve the purpose of corrosion protection. Preparation of conductive coating and Zn electrodeposited coating on the surface of grounding electrode is a hot research topic at present. Meanwhile, the process of Zn electrodeposited coating is simple and easy to operate, which has good uniformity and stable conductivity [7-11]. Therefore, Zn electrodeposited coating is more suitable for surface treatment of carbon steel as power grounding material. However, pure Zn coating has holes, crystal dislocations and other defects, and the defects often accelerate corrosion, resulting in the service life of pure Zn coating cannot reach the expectation. If other elements (such as Ni, W, P, etc.) or particles (such as SiC, ZrO₂ particles, etc.) are introduced into pure Zn coating, it will not only meet the requirements of conductivity, but also be expected to show excellent corrosion resistance [12-17]. Compared with pure Zn coating, composite coating has a higher value for surface protection of carbon steel as power grounding material.

In this paper, Zn-Ni alloy coating, Zn-Ni-W alloy coating and Zn-Ni-W/ZrO₂ composite coating are electrodeposited respectively on the surface of Q235 steel to achieve corrosion protection and make comparison which is innovative and significant. The corrosion of Q235 steel and different electrodeposited coatings was investigated through electrochemical testing and stray current corrosion experiment, so as to optimize the most suitable coating. It provides a new idea for improving the corrosion resistance of carbon steel as power grounding material.

2. EXPERIMENTAL

2.1 Materials and chemical agents

Q235 steel plate (6 cm × 3 cm × 0.3 cm) was cut as the experimental substrate. In the process of pretreatment, pure acetone, ethanol and hydrochloric acid were used. The samples were polished on both sides and then were sequentially immersed in acetone, ethanol and pure water for ultrasonic cleaning for 8 minutes to remove dust and oil on the surface of the samples. Finally, the samples were immersed in 15% hydrochloric acid for etching and activation for 2 minutes.

2.2 Preparation of different electrodeposited coatings

The pre-treated Q235 steel sample was used as the cathode, and electrolytic nickel plate was used as the anode to continuously provide nickel ions. During the electrodeposition process, the distance between cathode and anode was set as 3 cm. Different electrodeposited coatings were electrodeposited on the surface of Q235 steel sample, which were Zn-Ni alloy coating, Zn-Ni-W alloy coating and Zn-Ni-W/ZrO₂ composite coating respectively. The solution composition and electrodeposition parameters were shown in Table 1. Meanwhile, ZnCl₂, NiSO₄ and Na₂WO₄ were the main salts that can provide Zn²⁺, Ni²⁺ and WO₄²⁻ ions. H₃BO₃ and C₆H₁₄N₂O₇ were used as the buffering agent and complexing agent respectively during the electrodeposition process. Na₂SO₄ was used as the conducting salt to increase the conductivity of the solution. The pH value of the solution for preparing different electrodeposited coatings was adjust to 6.0 using 10% dilute hydrochloric acid or 1 mol/L sodium hydroxide. Different coatings were electrodeposited from 200 ml solution at the condition of 2 A/dm² current density and 60 °C temperature for 60 minutes.

Table 1. Solution composition and parameters for preparing different electrodeposited coatings

Different electrodeposited coatings	Solution composition	Electrodeposition parameters
Zn-Ni alloy coating	ZnCl ₂ 20 g/L, NiSO ₄ 32 g/L, C ₆ H ₁₄ N ₂ O ₇ 80 g/L, Na ₂ SO ₄ 26 g/L, H ₃ BO ₃ 30 g/L	temperature 60°C electrodeposition time 60 min
Zn-Ni-W alloy coating	ZnCl ₂ 20 g/L, NiSO ₄ 32 g/L, C ₆ H ₁₄ N ₂ O ₇ 80 g/L, Na ₂ SO ₄ 26 g/L, H ₃ BO ₃ 30 g/L, Na ₂ WO ₄ 20 g/L	temperature 60°C electrodeposition time 60 min
Zn-Ni-W/ZrO ₂ composite coating	ZnCl ₂ 20 g/L, NiSO ₄ 32 g/L, C ₆ H ₁₄ N ₂ O ₇ 80 g/L, Na ₂ SO ₄ 26 g/L, H ₃ BO ₃ 30 g/L, Na ₂ WO ₄ 20 g/L, nano-ZrO ₂ particles 10 g/L	temperature 60°C electrodeposition time 60 min

2.3 Testing methods

2.3.1 Surface morphology

The surface morphology of Q235 steel, Zn-Ni alloy coating, Zn-Ni-W alloy coating and Zn-Ni-W/ZrO₂ composite coating was characterized by SU-8010 scanning electron microscope. In order to improve the resolution and obtain clear images, different samples were sprayed with gold with a magnification of 5000 times. In addition, the three-dimensional surface profiles of different electrodeposited coatings were characterized by VK-250 laser microscope, and the surface roughness was measured.

2.3.2 Structure testing

The XRD diffraction patterns of Zn-Ni alloy coating, Zn-Ni-W alloy coating and Zn-Ni-W/ZrO₂ composite coating were detected by Philips X-ray diffraction instrument, and then introduced into Jade software to analyze the structure and phase composition. The X-ray diffractometer used Cu target K α rays with 40 kV voltage and 100 mA current. The diffraction angle range was 20°~80°, and the scanning rate was 4°/min.

2.3.3 Corrosion resistance performance

Simulated soil pore solution composed of 0.2 g/L sodium chloride, 0.015 g/L sodium bicarbonate, 0.08 g/L sodium sulfate, 0.12 g/L potassium nitrate and 0.06 g/L calcium chloride was prepared as the corrosion medium. The corrosion resistance of Q235 steel, Zn-Ni alloy coating, Zn Ni-W alloy coating and Zn-Ni-W/ZrO₂ composite coating in simulated soil pore solution was evaluated by electrochemical testing. Saturated calomel electrode was used as reference electrode, platinum electrode was used as auxiliary electrode, and different samples were used as working electrodes. The area of the working electrode exposed to the simulated soil pore solution was about 1 cm². Before testing of polarization curve and electrochemical impedance spectrum, the three electrode system was immersed in simulated soil pore solution for 1 h to obtain a stable open circuit potential. The scan rate of polarization curve was 1 mV/s, and the corrosion potential and corrosion current density were obtained by Tafel extrapolation method. The electrochemical impedance of samples was tested at the amplitude of 10 mV and frequency range of 100 kHz~10 mHz.

When Q235 steel was buried in the soil, in addition to the electrochemical corrosion, stray current corrosion may also occur. Therefore, the corrosion resistance of Q235 steel, Zn-Ni alloy coating, Zn-Ni-W alloy coating and Zn-Ni-W/ZrO₂ composite coating was further tested and evaluated by stray current corrosion experiment. The DC regulated power supply and different samples were buried in the soil with 20% water content. The DC stray current intensity was set as 15 mA. The morphology of different samples after 14 days of DC stray current corrosion was characterized by scanning electron microscopy.

3. RESULTS AND DISCUSSION

3.1 Surface morphology of different electrodeposited coatings

Figure 1 shows the surface morphology of Q235 steel and different electrodeposited coatings. It can be seen that the morphology characteristics of Zn-Ni alloy coating, Zn-Ni-W alloy coating and Zn-Ni-W/ZrO₂ composite coating are significantly different. As shown in Figure 1(b), the Zn-Ni alloy coating shows blocky structure with rough surface which is also reported by some researchers [18]. Zn-Ni-W alloy coating is composed of strip structure, and its compactness is obviously better than that of Zn-Ni alloy coating. Because the principle of Zn-Ni deposition is anomalous co-deposition, Zn

deposition takes precedence over Ni deposition. However, the principle of Zn-Ni-W deposition is that W deposition is induced during the anomalous co-deposition of Zn-Ni, which may cause lattice distortion and lead to changes in grain morphology, so as to improve the compactness of the coating. The anomalous co-deposition phenomenon of Zn-Ni is reported by some researcher [19-20]. As shown in Figure 1(d), the surface morphology of Zn-Ni-W/ZrO₂ composite coating shows spherical and granular structure which are tightly bonded. This is because ZrO₂ particles embedded in the grains gaps play the role of heterogeneous nucleation to accelerate the nucleation rate, which accelerates the formation rate of new crystal nuclei and impedes the growth of the formed crystal nuclei. In addition, ZrO₂ particles can also play a filling effect to achieve grain refinement. Therefore, Zn-Ni-W/ZrO₂ composite coating exhibits good compactness.

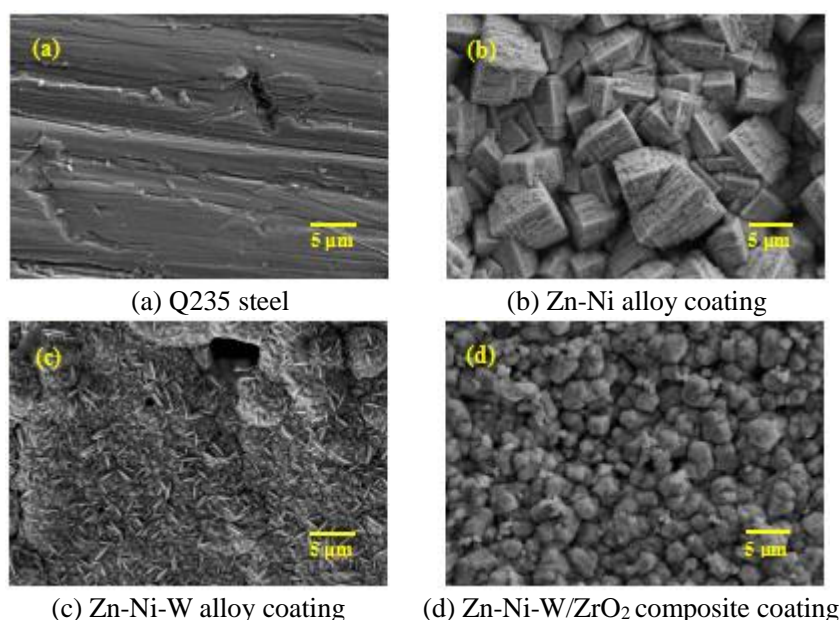
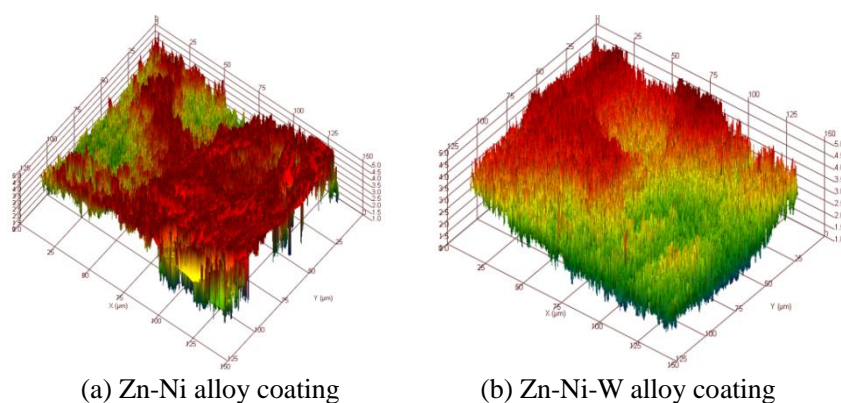


Figure 1. Surface morphology of Q235 steel and different electrodeposited coatings



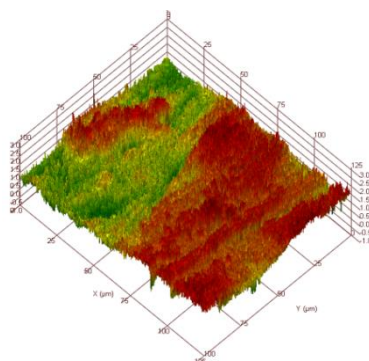
(c) Zn-Ni-W/ZrO₂ composite coating**Figure 2.** Three-dimensional surface profiles of different electrodeposited coatings

Figure 2 shows the three-dimensional surface profiles of different electrodeposited coatings. According to Figure 2(a), Figure 2(b) and Figure 2(c), Zn-Ni alloy coating, Zn-Ni-W alloy coating and Zn-Ni-W/ZrO₂ composite coating all present different surface roughness. The surface roughness of Zn-Ni-W/ZrO₂ composite coating is 0.526 μm, which is lower than that of Zn-Ni alloy coating (0.703 μm) and Zn-Ni-W alloy coating (0.619 μm). It is confirmed that Zn-Ni-W/ZrO₂ composite coating is relatively flat and compact.

3.2 Structure of different electrodeposited coatings

Figure 3 shows the XRD diffraction patterns of different electrodeposited coatings. According to the XRD diffraction patterns, Zn-Ni alloy coating, Zn-Ni-W alloy coating and Zn-Ni-W/ZrO₂ composite coating all show crystalline structure. The phase composition of Zn-Ni-W alloy coating is the same as that of Zn-Ni alloy coating, which contains elemental Zn phase and Ni₅Zn₂₁ phase, but there is no W-related phase. The reason is that W enter in the Ni lattice to form a substitutional solid solution with Ni as the solvent atom and W as the solute atom [21-22]. The phase composition of Zn-Ni-W/ZrO₂ composite coating contains ZrO₂ phase in addition to the elemental Zn phase and Ni₅Zn₂₁ phase. In the EDS spectrum of Zn-Ni-W/ZrO₂ composite coating shown in Figure 4, the characteristic peak of Zr element appears, which proves that a certain amount of ZrO₂ particles are doped in the composite coating. In view of the low doping amount of ZrO₂ particles, the conductive properties of the composite coating will not be significantly affected, but it is beneficial to refine the grains and improve the compactness of the composite coating. The effect of ZrO₂ particles on the surface morphology and grain size of materials has also been investigated by some researcher [23-24]. According to the Zr element distribution shown in Figure 4(b), it can be concluded that ZrO₂ particles are doped in the composite coating.

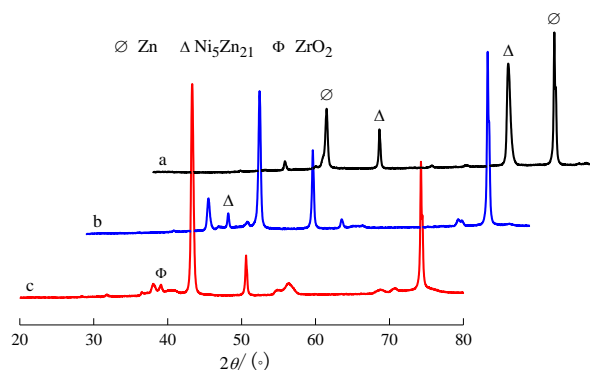


Figure 3. XRD diffraction patterns of different electrodeposited coatings: (a) Zn-Ni alloy coating; (b) Zn-Ni-W alloy coating; (c) Zn-Ni-W/ZrO₂ composite coating

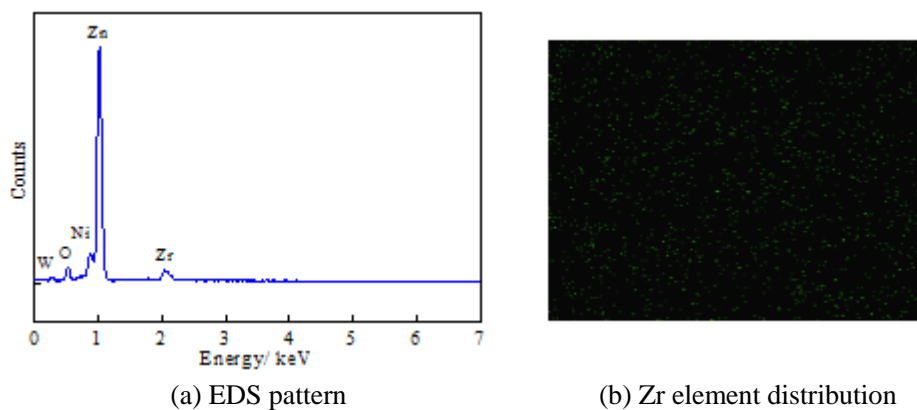


Figure 4. EDS pattern and Zr element distribution of Zn-Ni-W/ZrO₂ composite coating

3.3 Corrosion resistance of different electrodeposited coatings

3.3.1 Electrochemical corrosion

Figure 5 shows the polarization curves of Q235 steel and different electrodeposited coatings in simulated soil pore solution, and Table 2 lists the fitting results of polarization curves. By comparing the corrosion potential and corrosion current density, it is found that Zn-Ni alloy coating, Zn-Ni-W alloy coating and Zn-Ni-W/ZrO₂ composite coating can inhibit the anodic and cathodic reactions of Q235 steel in simulated soil pore solution to reduce the corrosion tendency and decrease the corrosion rate of Q235 steel. Compared with Q235 steel, the corrosion potential of Zn-Ni alloy coating, Zn-Ni-W alloy coating and Zn-Ni-W/ZrO₂ composite coating is increased by about 20 mV, 43 mV and 60 mV, respectively. The corrosion current density also correspondingly decreases. Some researcher point out that Zn-Ni alloy coating has good corrosion resistance due to the addition of nickel that affects the corrosion products during corrosion process [25-26]. Moreover, effect of tungsten on the corrosion resistance of alloy coatings has been reported in some papers [27-28]. According to the electrochemical corrosion theory, the lower the corrosion current density is, the better the corrosion resistance of the material has. Because Zn-Ni-W/ZrO₂ composite coating has the most positive corrosion potential of -0.485 V and the lowest corrosion current density of 9.87×10^{-7} A/cm², corrosion reaction is not easy to occur in simulated soil pore solution, and it has a better corrosion protection

effect on Q235 steel.

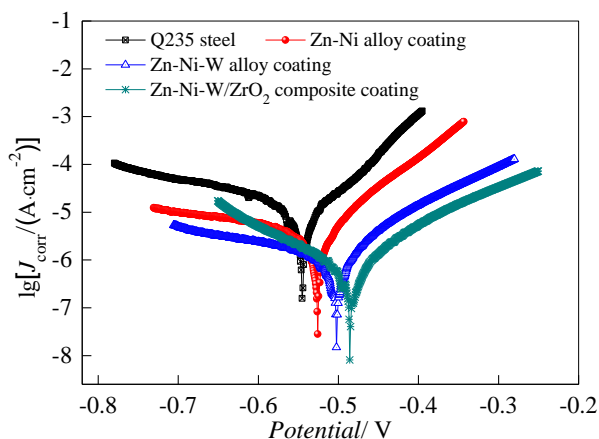


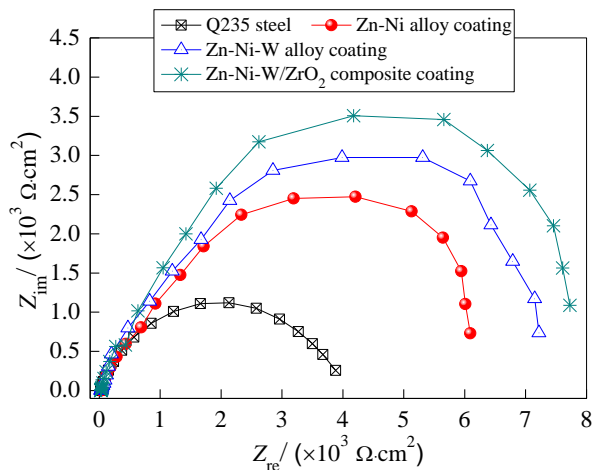
Figure 5. Polarization curves of Q235 steel and different electrodeposited coatings in simulated soil pore solution

Table 2. Fitting results of polarization curves

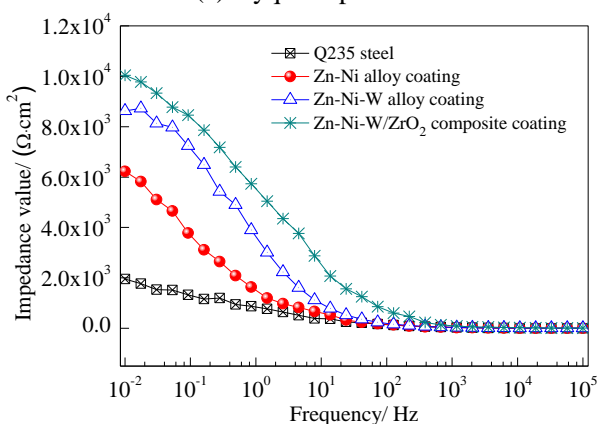
Different samples	Corrosion potential/ V	Corrosion current density/ (A·cm ²)
Q235 steel	-0.545	6.10×10 ⁻⁵
Zn-Ni alloy coating	-0.526	4.06×10 ⁻⁶
Zn-Ni-W alloy coating	-0.502	1.89×10 ⁻⁶
Zn-Ni-W/ZrO ₂ composite coating	-0.485	9.87×10 ⁻⁷

Figure 6 shows the electrochemical impedance spectra of Q235 steel and different electrodeposited coatings in simulated soil pore solution. Generally, capacitive reactance, charge-transfer resistance and impedance value of low frequency are used to evaluate the corrosion resistance of the coating and protection effect on the substrate [29-30]. The coating with larger capacitive reactance and higher charge-transfer resistance has better corrosion resistance.

According to Figure 6(a) and Figure 6(b), it can be seen that Q235 steel has the smallest capacitive reactance, and the charge-transfer resistance and low-frequency impedance values are only 3.69×10³ Ω·cm² and 2.95×10³ Ω·cm² respectively. However, Zn-Ni-W/ZrO₂ composite coating has the largest charge-transfer resistance and the highest low-frequency impedance which are 7.34×10³ Ω·cm² and 1.01×10⁴ Ω·cm² respectively.



(a) Nyquist spectra



(b) Bode spectra

Figure 6. Electrochemical impedance spectra of Q235 steel and different electrodeposited coatings in simulated soil pore solution

From the analysis above, the compactness of Zn-Ni-W alloy coating prepared by introducing W element into the Zn-Ni alloy coating is improved, which prevents the corrosive ions in simulated soil pore solution from penetrating into the coating and effectively inhibits the corrosion reaction of Q235 steel. Therefore, the corrosion protection of Zn-Ni-W alloy coating on Q235 steel in simulated soil pore solution is better than that of Zn-Ni alloy coating. However, Zn-Ni-W/ZrO₂ composite coating has more compact surface with nodular structures, which can better prevent the corrosive ions in simulated soil pore solution from contacting Q235 steel. In addition, Zn-Ni-W/ZrO₂ composite coating is uniformly doped with nano-ZrO₂ particles with high chemical stability, which improves the corrosion resistance of the composite coating. Therefore, Zn-Ni-W/ZrO₂ composite coating plays a better role in protecting Q235 steel in simulated soil pore solution.

3.3.2 Stray current corrosion

Figure 7 shows the surface morphology of Q235 steel and different electrodeposited coatings after 14 days of corrosion under the condition of 15 mA DC stray current. As can be seen from Figure

7(a), the corroded morphology of Q235 steel is very different from the original morphology. Corrosion products are accumulated on the surface and disorderly cracks are formed, indicating that Q235 steel is seriously corroded. The corrosion mechanism and damage characteristic of Q235 steel under the effect of stray current are studied in some literatures [31-32].

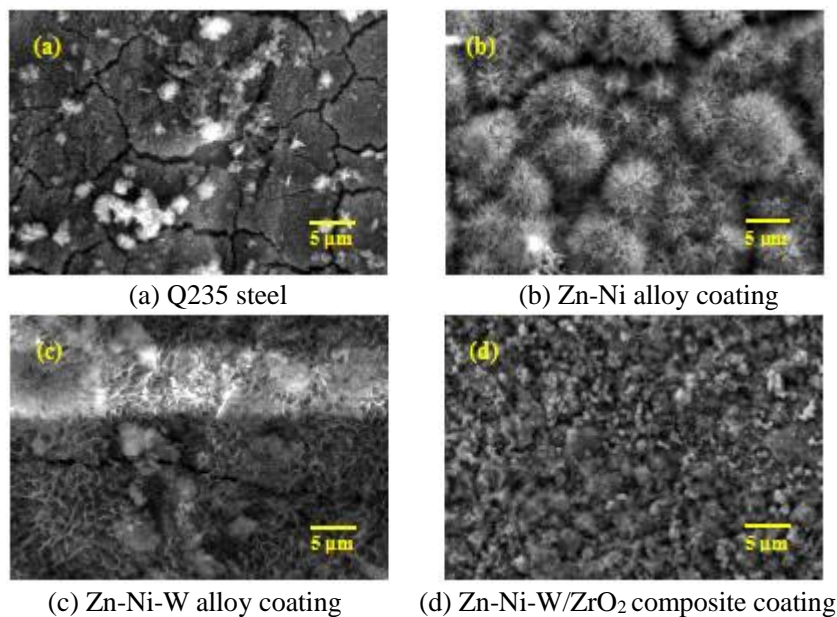


Figure 7. Surface morphology of Q235 steel and different electrodeposited coatings after 14 days of corrosion under the condition of 15 mA DC stray current

According to Figure 7(b), Figure 7(c) and Figure 7(d), it can be seen that after 14 days of corrosion under the condition of 15 mA DC stray current, Zn-Ni alloy coating is corroded, resulting in the transformation from the blocky-shape to spherical shape. Local accumulation of corrosion products and formation of cracks in Zn-Ni-W alloy coating will induce corrosive ions in the simulated soil pore solution to penetrate into the coating. With the further extension of DC stray current corrosion time, the corrosion degree of Zn-Ni-W alloy coating will be aggravated. Zn-Ni-W/ZrO₂ composite coating still maintains integrity and good compactness. The corrosion degree of Zn-Ni-W/ZrO₂ composite coating is lighter than that of Zn-Ni alloy coating and Zn-Ni-W alloy coating. Zn-Ni-W/ZrO₂ composite coating with good compactness can prevent the contact between the corrosive medium and the Q235 steel to cut off the corrosion channel, thus inhibiting the corrosion reaction and improving the corrosion resistance of Q235 steel under the combined action of electrochemical corrosion and stray current corrosion. Some researcher also prove that the ZrO₂ particles can effectively improve the corrosion resistance of metal coatings [33-34].

4. CONCLUSIONS

(1) Zn-Ni alloy coating, Zn-Ni-W alloy coating and Zn-Ni-W/ZrO₂ composite coating all can inhibit the corrosion process of Q235 steel in simulated soil pore solution, so as to improve the corrosion resistance of Q235 steel. Compared with Zn-Ni alloy coating and Zn-Ni-W alloy coating,

Zn-Ni-W/ZrO₂ composite coating has the lowest corrosion current density of 9.87×10^{-7} A/cm², the highest charge-transfer resistance of 7.34×10^3 Ω·cm² and the largest low-frequency impedance of 1.01×10^4 Ω·cm² in simulated soil pore solution. After 14 days of corrosion under the condition of 15 mA DC stray current, the surface morphology of Zn-Ni-W/ZrO₂ composite coating still maintains compact with lightest corrosion degree.

(2) Zn-Ni-W/ZrO₂ composite coating has good compactness which prevents the corrosive medium from contacting the Q235 steel substrate. In addition, Zn-Ni-W/ZrO₂ composite coating is uniformly doped with ZrO₂ particles with high chemical stability, which improves the corrosion resistance of the composite coating. Therefore, electrodeposition of Zn-Ni-W/ZrO₂ composite coating can not only meet the requirements of power grounding material, but also significantly improve the corrosion resistance of carbon steel under the combined action of electrochemical corrosion and stray current corrosion in simulated soil pore solution.

References

1. L. Liu, J. J. Li, M. X. Peng, W. B. Li, B. Lei and G. Z. Meng, *Eng. Fail. Anal.*, 135 (2022) 106136.
2. H. Z. Hu, M. G. Fang, F. Y. Hu, S. L. Zeng and X. F. Deng, *Electr. Power Syst. Res.*, 195 (2021) 107174.
3. J. R. Zhang, L. N. Xu and Q. X. Zhao, *Constr. Build. Mater.*, 145 (2017) 347.
4. C. J. Lu, L. F. Li, Z. X. Liu, C. B. Xu, M. Y. Xin, G. Q. Fu, T. Wang and X. Wang, *Measurement*, 199 (2022) 111469.
5. Z. L. Zhang, D. J. Mei, Y. H. Dan, J. Zou, G. H. Liu and C. F. Gao, *Electr. Power Syst. Res.*, 178 (2020) 106049.
6. Z. L. Zhang, H. R. Ye, Y. H. Dan, Z. Duanmu, J. Deng, C. F. Gao and P. F. Gan, *Measurement*, 166 (2020) 108213.
7. S. Rossi, M. Pinamonti and M. Calovi, *Case Stud. Constr. Mater.*, 17 (2022) 01257.
8. M. S. Darris, A. Hossain, A. M. Asha, R. K. Manavalan, J. Ahmed and S. M. A. Shibli, *Ceram. Int.*, 27 (2022) 102247.
9. C. X. Lin, Y. C. Liu, X. X. Zhang, X. F. Miao, Y. Q. Chen, S. J. Chen and Y. N. Zhang, *J. Power Sources*, 549 (2022) 232078.
10. Y. H. Cui, Q. H. Zhao, X. J. Wu, Z. J. Wang, R. Z. Qin, Y. T. Wang, M. Q. Liu, Y. L. Song, G. Y. Qian, Z. B. Song, L. Y. Yang and F. Pan, *Energy Storage Mater.*, 27 (2020) 1.
11. Y. D. Yu, G. Y. Wei, J. W. Lou, H. L. Ge, L. X. Sun and L. Z. Zhu, *Surf. Eng.*, 29 (2013) 234.
12. P. Behera, S. K. Rajagopalan, S. Brahim, C. A. Venturella, S. P. Gaydos, R. J. Straw and S. Yue, *Surf. Coat. Technol.*, 417 (2021) 127181.
13. K. Foster, J. Claypool, W. G. Fahrenholtz, M. O. Keefe, T. Nahlawi and F. Almodovar, *Thin Solid Films*, 735 (2021) 138894.
14. C. Muller, M. Sarret and M. Benballa, *Surf. Coat. Technol.*, 162 (2003) 49.
15. R. Q. Li, Q. J. Dong, J. Xia, C. H. Luo, L. Q. Sheng, F. Cheng and J. Liang, *Surf. Coat. Technol.*, 366 (2019) 138.
16. Z. Q. Liao, F. P. Zhong, Z. Q. Zhang, L. Jiang, G. Y. Wei, M. Yuan and L. L. Ren, *Mater. Today Commun.*, 33 (2022) 104769.
17. Y. H. Hu, Y. D. Yu, H. L. Ge, G. Y. Wei and L. Jiang, *Int. J. Electrochem. Sci.*, 14 (2019) 1649.
18. E. M. D. Oliveira and I. A. Carlos, *Surf. Coat. Technol.*, 206 (2011) 250.
19. Y. D. Yu, Y. Cao, M. G. Li, G. Y. Wei and H. Dettinger, *Mater. Res. Innovations*, 18 (2014) 314.
20. C. Srivastava, S. K. Ghosh, S. Rajak, A. K. Sahu, R. Tewari, V. Kain and G. K. Dey, *Surf. Coat.*

- Technol.*, 313 (2017) 8.
21. J. C. Tang, J. J. Niu, C. W. Yang, S. Rajendran, Y. P. Lei, M. Sawangphruk, X. Y. Zhang and J. Q. Qin, *Fuel*, 330 (2022) 125510.
 22. M. Y. Wang, Z. Wang and Z. C. Guo, *Mater. Chem. Phys.*, 148 (2014) 245.
 23. Z. G. Wang, J. H. Ouyang, Y. H. Ma, Y. J. Wang, L. Y. Xie, Z. G. Liu, A. Henniche and Y. Wang, *Ceram. Int.*, 45 (2019) 14297.
 24. N. Garg, S. Bera and S. Velmurugan, *Thin Solid Films*, 670 (2019) 60.
 25. B. Abedini, N. P. Ahmadi, S. Yazdani and L. Magagnin, *Surf. Coat. Technol.*, 372 (2019) 260.
 26. H. M. Lateef, A. R. E. Sayed and H. S. Mohran, *T. Nonferr. Metal Soc.*, 25 (2015) 2807.
 27. X. P. Zhang, L. M. Lai, S. M. Xiao, H. J. Zhang, F. F. Zhang, N. Li and S. F. Guo, *Intermetallics*, 143 (2022) 107485.
 28. P. F. Sun, D. Z. Wang, W. J. Song, C. W. Tang, J. X. Yang, Z. D. Xu, Q. W. Hu and X. Y. Zeng, *Surf. Coat. Technol.*, 452 (2023) 129079.
 29. A. M. K. Kirubaharan, A. Anderson, K. G. Saravanan, M. Rahasekaramoorthy and R. Balachandar, *Mater. Today: Proc.*, 33 (2020) 902.
 30. C. S. Ni, L. Y. Lu, C. L. Zeng and Y. Niu, *J. Power Sources*, 261 (2014) 162.
 31. J. G. Feng, Z. G. Chen, C. Wu, C. K. Qin and X. S. Wei, *Process Saf. Environ. Prot.*, 164 (2022) 38.
 32. C. T. Wang, W. Li, Y. Q. Wang, X. F. Yang and S. Y. Xu, *Constr. Build. Mater.*, 247 (2020) 118562.
 33. J. L. Yang, A. Y. Chen, F. Liu, L. J. Gu, X. F. Xie and Z. Y. Ding, *Ceram. Int.*, 48 (2022) 35280.
 34. E. Kennedy, B. S. Sachin, M. amachandra, C. A. Niranjana, N. Sriraman, V. K. S. Jain and N. S. Narayanan, *Mater. Today: Proc.*, 39 (2021) 1710.

© 2022 The Authors. Published by ESG (www.electrochemsci.org). This article is an open access article distributed under the terms and conditions of the Creative Commons Attribution license (<http://creativecommons.org/licenses/by/4.0/>).